




Proceeding Paper

Influence of Multiwalled Carbon Nanotubes in Sulfur/Carbon Nanotube Composites Synthesized Using Solution Casting Method [†]

Karishma Jain ¹, Sushil Kumar Jain ^{1,*} , Anu Malhotra ², Shalini Dixit ² , Balram Tripathi ^{2,*}  and Rajesh Sahu ³

¹ Department of Physics, School of Basic Sciences, Manipal University Jaipur, Jaipur 303007, India; karishma.221051026@muj.manipal.edu

² Department of Physics, S. S. Jain Subodh PG (Auto.) College, Jaipur 302004, India; anumalhotrachd@gmail.com (A.M.); shaliniyitwari@gmail.com (S.D.)

³ Centre for Renewable Energy and Storage, Suresh Gyan Vihar University, Jaipur 302017, India; rajeshsahuphysics@gmail.com

* Correspondence: sushilkumar.jain@jaipur.manipal.edu (S.K.J.); balramtripathi1181@gmail.com (B.T.); Tel.: +91-9828034055 (S.K.J.); +91-9460067015 (B.T.)

[†] Presented at the International Conference on Recent Advances in Science and Engineering, Dubai, United Arab Emirates, 4–5 October 2023.

Abstract: In this manuscript, we are reporting on the influence of MWNTs (multiwalled carbon nanotubes) on the structural, bonding, and surface morphological response on sulfur nanoparticles. Sulfur and multiwalled carbon nanotube (MWCNT) composites are formed using the solution casting method. The concentration of MWCNTs (0.01 and 0.05) and sulfur (0.99 and 0.95), respectively, was taken in weight ratios during fabrication of the composites. These fabricated composites have been characterized using XRD (X-ray diffraction), FESEM (field emission scanning electron microscopy), and FTIR (Fourier-transform infrared spectroscopy) techniques. XRD spectra reveal that the crystallite size distribution was in the range of ca. 55 nm to 78 nm, as well as enhanced crystallinity upon increasing the concentration of MWCNTs in sulfur composites. Dislocation density and strain have been found to be increased in composites showing increased augmentation of MWCNTs (i.e., S95% MWCNT5%), while FESEM images confirm the uniform distribution of MWCNTs in sulfur composites, along with round structures at the nanoscale range. FTIR spectra depicted the bending and stretching of C-H bands. Composites with a higher concentration of MWCNTs show slightly more stretching vibrations. This indicates the further delocalization of electrons, which reveals that as MWCNTs' concentration is increased, electrical conductivity enhances, showing that MWCNTs could perform better in electrical industries. The further delocalization of electrons also expresses that free electron–hole pair formation is better in composites with a higher concentration of MWCNTs, accounting for the fact that the photocatalytic response may increase in composites with a higher concentration of MWCNTs. Overall, it can be said that as the MWCNT concentration is ameliorated, the composites show a more crystallized structure with more vibrations. This characteristic of MWCNTs/sulfur composites is useful in photocatalytic response as well as in cathode materials in sulfur batteries.

Keywords: multiwalled carbon nanotube; sulfur; solution casting method; delocalization; tensile strain



Citation: Jain, K.; Jain, S.K.; Malhotra, A.; Dixit, S.; Tripathi, B.; Sahu, R. Influence of Multiwalled Carbon Nanotubes in Sulfur/Carbon Nanotube Composites Synthesized Using Solution Casting Method. *Eng. Proc.* **2023**, *59*, 217. <https://doi.org/10.3390/engproc2023059217>

Academic Editors: Nithesh Naik, Rajiv Selvam, Pavan Hiremath, Suhas Kowshik CS and Ritesh Ramakrishna Bhat

Published: 25 January 2024



Copyright: © 2024 by the authors. Licensee MDPI, Basel, Switzerland. This article is an open access article distributed under the terms and conditions of the Creative Commons Attribution (CC BY) license (<https://creativecommons.org/licenses/by/4.0/>).

1. Introduction

Carbon nanotubes (CNTs) have gained immense attention due to their activity against chemical and biological pollutants [1]. CNTs are regarded for their higher area-to-volume ratio, higher thermal, electrical, and mechanical abilities, and low density [2]. John Raphael et al. reported that adding CNTs to form composites could increase the load-carrying capacity or the strength of the overall nanomaterial. Apart from this, CNTs lessen weight

and behave as heat conductors [2]. They are hydrophobic in nature; to ameliorate dispersibility, they can be functionalized using nitric acid. MWCNTs are crystalline in nature and are tubular allotropic forms of elemental carbon and can be utilized as an additive to support catalysts utilized in organic transformations [3]. MWCNTs are composed of many layers of graphite wrapped around each other in a cylindrical way, possessing an interlayer dispersing of 3.4 Angstroms [4]. Ilyas Raza et al. studied why carbon nanotubes are known to be used as conductive nanofillers to ameliorate mechanical and physical properties [5]. The size of CNTs plays a key role in achieving materials strengthening [5]. Generally, in polar solvents, CNTs can agglomerate due to Van der Waals inter tube binding, which can reach 500 eV per micrometer [6]. To prevent this situation, solvents are chosen appropriately, for instance CHP (cyclohexyl-pyrrolidone) and dimethylformamide (DMF). The latter might vitiate the structure of SWCNTs (single-walled carbon nanotubes). A. K. Singha Deb et al. found that because of CNTs' hydrophobicity and chemical inertness, their use is limited. Henceforth, they are intercalated with covalent or non-covalent changes. Covalent surface transformations include the intercalation of new elements (viz., sulfur, nitrogen, fluorine), or biomolecules could be infused. Non-covalent surface transformation includes the adsorption of surfactants, polymers, or biological macromolecules. That is to say that their intrinsic structure does not change. The covalent surface transformation method is said to have better control than its counterpart [1]. Toshihiko Fujimori et al. proposed that SWCNTs have fluctuating behavior, from metallic to semiconducting, which relies on nanotube chirality (mentioned from the diameter to orientation along the axis). Apart from this, CNTs are intensely rigid as they have stable sp^2 carbon bonds [7]. Jamshed Aftab et al. investigated that after merging MWCNTs with binary composite WO_3/WS_2 , the specific capacity and conductivity of the electrode enhanced. As a result, the ternary asymmetric supercapacitor was used for practical implementation [8]. M. Isacfranklin et al. introduced that CNTs are fruitful alternatives for energy storage devices due to their good mechanical strength, and concentric tubes in MWCNTs help in imparting support to other compounds [9]. Sulfur is implemented in making cathode in lithium sulfur batteries on account of its abundance in nature, cost effectivity, high theoretical energy density, environmental friendliness, and its ability to hold more energy compared to traditional ion-based batteries. Sulfur and MWCNTs both have their dominance in electrical purposes. That is why the influence of MWCNTs on sulfur/MWCNT composites has been studied in this paper.

2. Materials and Method

2.1. Materials

Sulfur powder (99.99% purity) was purchased from Rankem Avantor Performance Materials India Limited. Carboxyl group functionalized MWCNTs were purchased from the Chengdu Institute of organic Chemistry, Chinese Academy of Sciences (China). Two compositions were formed using a solution casting method. Sulfur with 95% parts (in weight) and MWCNTs with 5% parts (in weight) are named S95%MWCNT5%. Correspondingly, sulfur with 99% parts (in weight) and MWCNTs with 1% part (in weight) are named S99%MWCNT1%. MWCNTs were dissolved in 10 mL ethanol and sonicated for an hour using a probe sonicator. Sulfur was dissolved in 30 mL ethanol and magnetically stirred for an hour at 345 rpm. The two solutions were mixed. The whole mixture was then sonicated for 30 min again using a probe sonicator until attaining a uniform dispersion. After filtering the residue, it was then vacuum-dried for one day at room temperature. The mixtures were then crushed using a pestle and mortar for an hour. Figure 1 represents the schematic diagram of the synthesis procedure for sulfur and MWCNT composites. The experiment was performed at 28 °C.

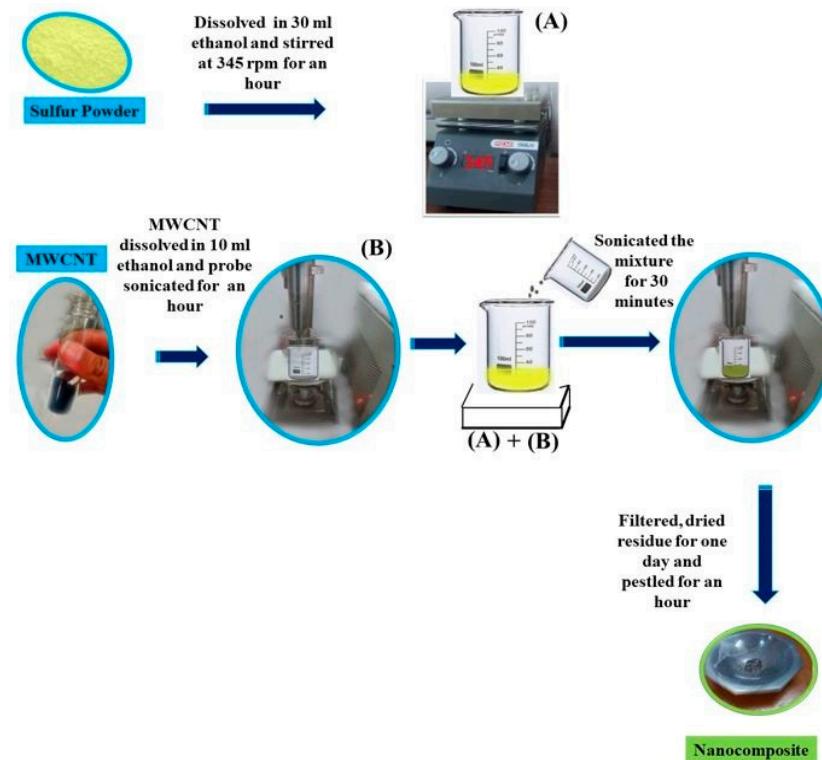


Figure 1. Schematic diagram for synthesis procedure of sulfur and MWCNT composites.

2.2. Characterization

Structural analysis of the nanocomposites was performed using the Bruker-AXS D8 ADVANCE X-ray diffractometer with a $\text{CuK}\alpha$ radiation source with a step width of 0.02° and scan range of 5° to 75° , and it operated at a voltage of 40 kV and current of 50 mA. The scan speed was $10.00^\circ/\text{min}$. The XRD machine offers less than 380 eV FWHM energy resolution for Cu—radiation at 298 K. Surface morphology of the composites was investigated using MIRA II LMH scanning electron microscopy (SEM) from TESCAN using an accelerating voltage of 5 kV; after, gold-coating occurred with apparatus DII—29030SCTR Smart Coater. The Bruker Alpha Fourier-transform infrared (FT-IR) spectrometer in the range 4000 cm^{-1} to 400 cm^{-1} was used to collect the FTIR spectra using the KBr pellet sample handling technique.

3. Results and Discussion

3.1. XRD Diffractogram Studies

The sulfur in the composites resembles sulfur with JCPDS No. 77-0145. Figure 2 depicts the XRD spectra for composites (a) S99% MWCNT1% and (b) S95% MWCNT 5%. Table 1 depicts the estimated values of strain, dislocation density, and crystallite size obtained using the Debye–Scherrer method (DS), modified Scherrer method (MS), and WH-Plot (WH) for (1) S99% MWCNT1% and (2) S95% MWCNT5% composites.

From Table 1, it can be inferred that for composite S99% MWCNT1%, the average crystallite size ranges from 58 nm to 67 nm, and for composite S95% MWCNT5%, the average crystallite size ranges from approximately 55 nm to 78 nm. Also, the tensile strain and dislocation density increased slightly upon introducing the augmented MWCNT concentration. This increased strain reveals that the mechanical strength increased in the composite with a higher concentration of MWCNTs, which unveils that this composite with a higher MWCNT concentration may prove to be better in battery applications. The increase in dislocation density suggests the occurrence of enhanced strength in the composite with a higher MWCNT concentration, again suggesting better electrode applications. Figure 3

illustrates the WH-Plot for (a) S99% MWCNT1% and (b) S95% MWCNT5%. The slope of WH- Plot represents strain.

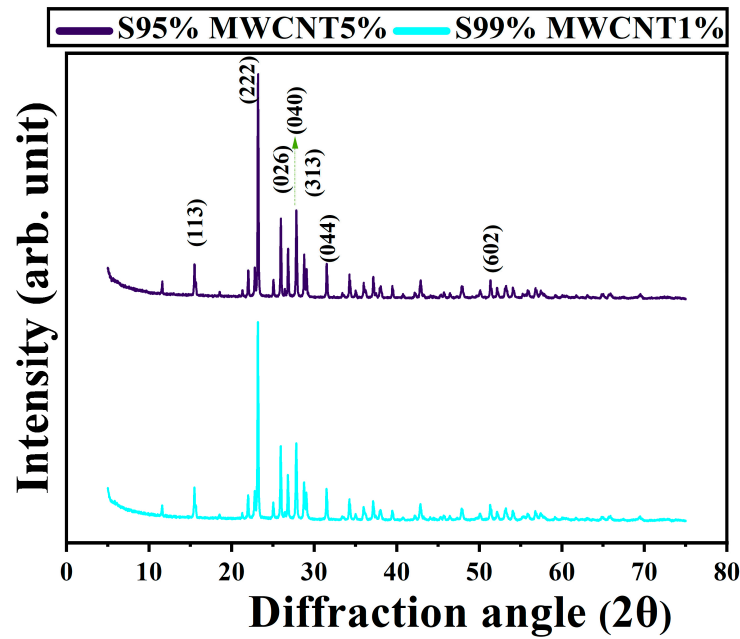


Figure 2. XRD spectra for S99% MWCNT1% and S95% MWCNT5%.

Table 1. Estimated values of strain, dislocation density, and crystallite size (*t*) obtained using the Debye–Scherrer method (DS), modified Scherrer method, (MS) and WH-Plot (WH) for (1) S99% MCNT1% and (2) S95% MWCNT5%.

Sr. No.	Sample Name	Strain ($\epsilon \times 10^{-4}$)	Dislocation Density (δ) (10^{-4} nm^{-2})	Crystallite Size t_{DS} (in nm)	Crystallite Size t_{MS} (in nm)	Crystallite Size t_{WH} (in nm)
1.	S99% MWCNT 1%	3.74	2.96	58.92	64.75	67.64
2.	S95% MWCNT 5%	8.70	3.35	55.17	64.90	78.34

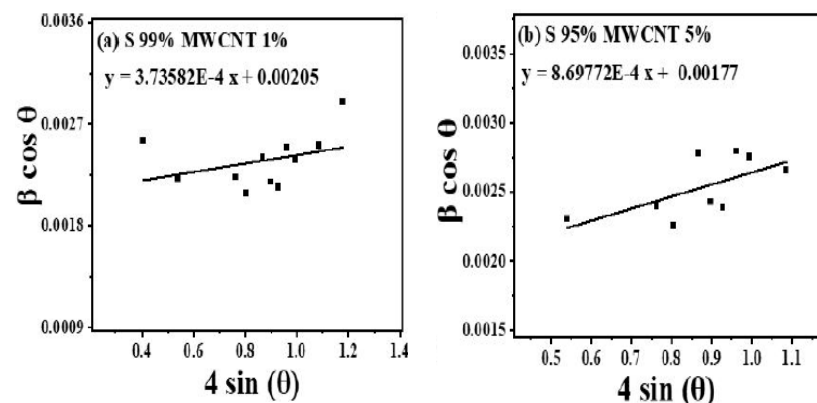


Figure 3. W-H Plot for (a) S99% MWCNT1% and (b) S95% MWCNT5%.

Figure 4 illustrates a column chart depicting the crystallinity (in %) of composites (a) S99% MWCNT1% and (b) S95%MWCNT5%. From Figure 4, it can be seen that S99% MWCNT1% composite’s crystallinity is at 51.82%, and S95% MWCNT5% composite’s crystallinity is at 55.78%. Also, as the MWCNT concentration increases, crystallinity

increases. In other words, the augmentation of MWCNTs enhances crystalline nature. The increase in crystallinity indicates an increase in long range order, which in turn increases the strength of the composites with a higher concentration of MWCNTs. This reflects the property of MWCNT, that despite it being added in small amounts, it has strengthened the composite.

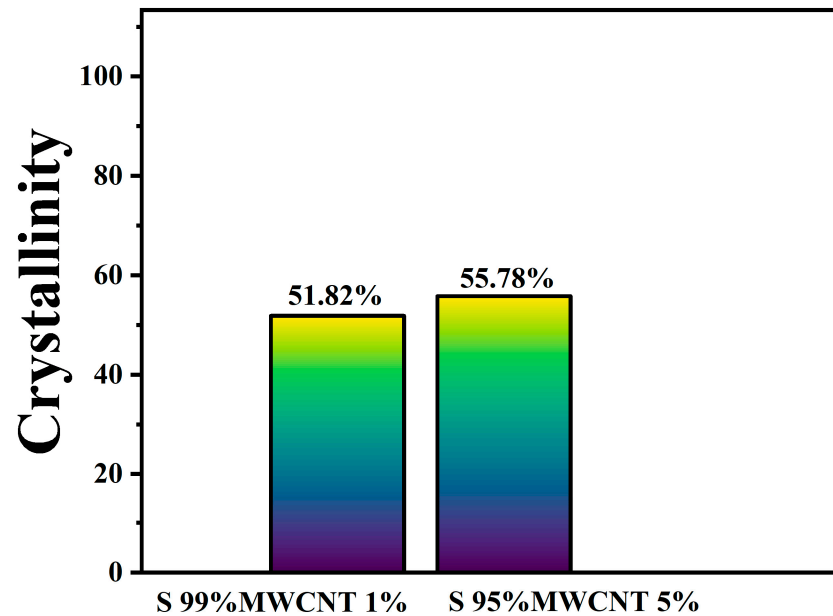


Figure 4. Column chart depicting crystallinity (in %) of composites—S99% MWCNT1% and S95% MWCNT5%.

3.2. Morphological Studies

Figure 5A,B represent the FESEM micrographs of (A) S 95% MWCNT 5% and (B) S 99% MWCNT 1%. Figure 6A represents a magnified view at 100 nm of S 95% MWCNT 5%. Alongside, Figure 6B represents the counts vs. size (nm) histogram curve for Figure 6A. In Figure 5A,B, composite particles appear to be round, with some degree of agglomeration. MWCNTs have fibrous structures, and sulfur has a round structure. Figure 6A represents mixed fiber/round morphologies. The particle size calculated from Figure 6B shows an average particle size of 46.45 nm.

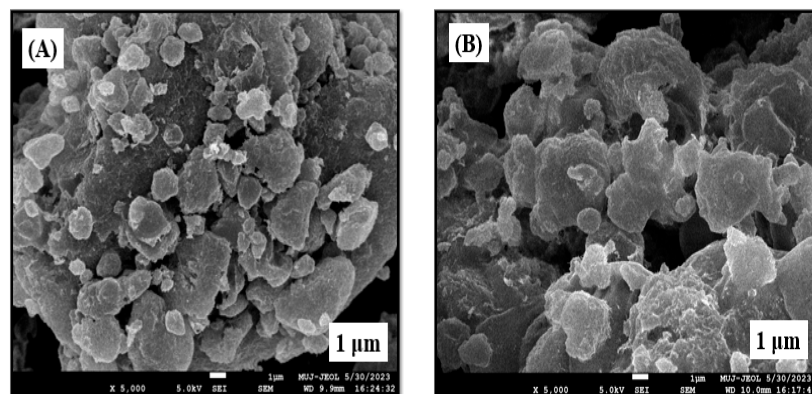


Figure 5. FESEM micrographs—(A) S95% MWCNT5% and (B) S99% MWCNT1%.

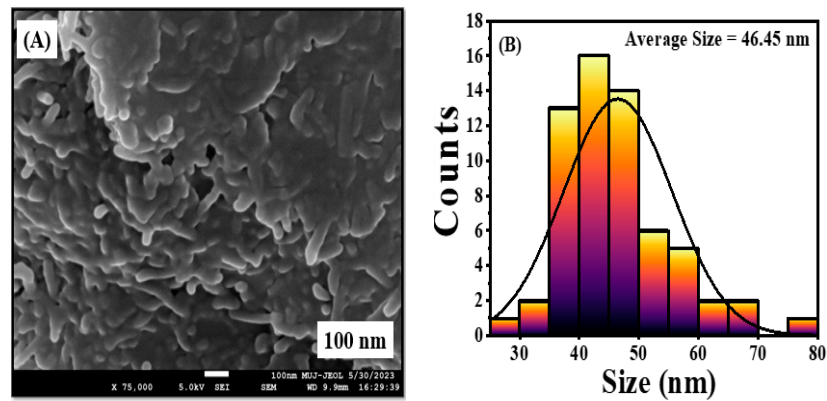


Figure 6. (A) represents FESEM micrograph of S 95% MWCNT 5% at magnified view at 100 nm. (B) represents counts vs. size (nm) histogram curve.

3.3. FTIR Studies

FTIR interpretation is mainly performed with the help of “*Infrared Spectroscopy: Fundamentals and Applications*” a book written by Barbara Stuart [10]. Figure 7 shows the KBr-FTIR interferogram of (a) S95% MWCNT5% and (b) S99% MWCNT1%. Table 2 shows the approximate characteristics of the vibrations and corresponding wave numbers related to the transmittance peak in the IR spectrum. The FTIR lines for both the composites have the same peak positions. It is observed that at 1045 cm^{-1} , composite S95% MWCNT 5% has a higher peak than S99% MWCNT 1%, which is also shown in the inset graph. This 1045 cm^{-1} peak is associated with the C-O stretching band of alcohols and S=O stretching of sulfur compounds. The inset graph is a superposition of two FTIR lines. The stronger band also signifies the further delocalization of electrons. This phenomenon tends to increase electrical conductivity [11]. Also, this delocalization indicates further free exciton pairs generation, accounting for the fact that the photocatalytic response could increase in the composite with a higher concentration of MWCNTs.

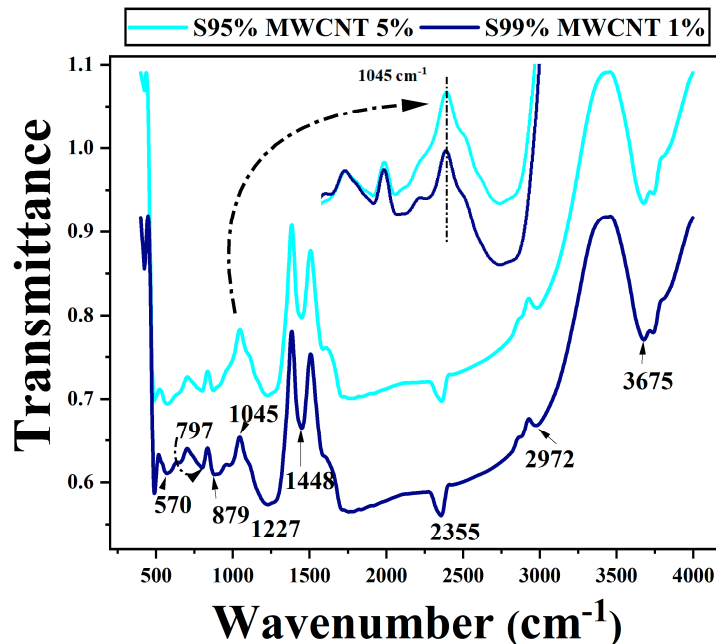


Figure 7. KBr-FTIR interferogram for S95% MWCNT5% and S99% MWCNT1%.

Table 2. Approximate characteristics of the vibrations and corresponding wave numbers related to transmittance peak in the KBr-FTIR spectrum for (a) S95% MWCNT5% and (b) S99% MWCNT1%.

Sr. No.	Position of Bands (cm ⁻¹)	Assignment of Bands
1	570	C-H out-of-plane bending, =C-H out-of-plane bending in alkenes
2	797	C-H out-of-plane bending of aromatic compounds, =C-H out-of-plane bending in alkenes [12]
3	879	S-OR ester group [12]
4	1045	C-O stretching band of alcohols, S=O stretching of sulfur compounds [13]
5	1227	Aliphatic C-O stretching of esters
6	1448	C=C stretching of carboxylic acid [14]
7	2355	Combination C-H stretching [15]
8	2972	C-H stretching of alkane [14]
9	3675	O-H stretching of alcohol [15]

4. Conclusions

In summary, MWCNT/sulfur composites have been synthesized using a solution casting method. The XRD spectra confirm the crystalline structure of the composites. Crystallinity has been found to increase with the augmented MWCNT concentration. The strain and dislocation density ameliorate as the MWCNT concentration increases. The average crystallite size distribution was found in the range of (ca. 55 nm to 78 nm). The surface morphology confirms the homogeneous distribution of MWCNTs in sulfur, along with round structures for the composites. The fiber-like structure resemblance is due to the presence of MWCNTs, and round structures are due to sulfur. The FT-IR interferogram depicts the presence of =C-H, C-OH, C=O, S=O, C-H, S-OR, O-H, C=C, and C-O bonding vibrations. Crystallinity has been found to increase upon enhancing the MWCNT concentration in sulfur composites.

Author Contributions: Conceptualization: S.K.J. and B.T.; methodology: S.K.J. and B.T.; software: K.J.; validation: K.J. and A.M.; formal Analysis: K.J.; investigation: K.J.; resources: B.T. and S.D.; data curation: S.K.J. and B.T.; writing—original draft preparation: K.J.; writing—review and editing: S.K.J. and B.T.; visualization: R.S.; supervision: S.K.J. and B.T.; project administration: S.K.J. and B.T.; funding acquisition: K.J. and S.K.J. All authors have read and agreed to the published version of the manuscript.

Funding: Financial support was received from Ramdas Pai Scholarship granted by Manipal University Jaipur.

Institutional Review Board Statement: Not applicable.

Informed Consent Statement: Not applicable.

Data Availability Statement: The datasets for the present study are available from the corresponding author on reasonable request.

Acknowledgments: We are grateful to the Central Analytical Facility (CAF) for FTIR studies. We are also thankful to the Sophisticated Analytical Instrument Facility (SAIF), Manipal University Jaipur for FESEM and XRD characterizations. Priyanka Kumari, Vipul Sharma, and Moti Kumar Jha (Scientific Officer) from Manipal University Jaipur are also acknowledged for their relevant suggestions and input in the present research work. Jagmohan Lal Sharma, R.R.B.M. University Alwar also contributed to the initial stages of this research work.

Conflicts of Interest: The authors declare no conflicts of interest.

References

1. Deb, A.K.S.; Dhume, N.; Dasgupta, K.; Ali, S.M.; Shenoy, K.T.; Mohan, S. Sulfur Ligand Functionalized Carbon Nanotubes for Removal of mercury from wastewater—experimental and density functional theoretical study. *Sep. Sci. Technol.* **2019**, *54*, 1573–1587. [CrossRef]
2. Raphael, J.; Bhat, A.G.; Siby, J.; Geevarghese, B.D.; George, N.; Chacko, T. Mechanical buckling of nanocomposites: Experimental and numerical investigations. *Polym. Polym. Compos.* **2021**, *29*, 1313–1324. [CrossRef]
3. Minchitha, K.U.; Rekha, M.; Nagaraju, N.; Kathyayini, N. Evaluation of Catalytic Activity of Acid Activated Multiwalled Carbon Nanotubes in an Esterification Reaction. *Curr. Catal.* **2014**, *4*, 20–30. [CrossRef]
4. Bhatt, A.; Jain, A.; Gurnany, E.; Jain, R.; Modi, A.; Jain, A. *Carrier for Drug Delivery*; Elsevier Inc.: Amsterdam, The Netherlands, 2016; pp. 465–501.
5. Raza, I.; Hussain, M.; Khan, A.N.; Katzwinkel, T.; Feldhusen, J. Properties of Light Weight Multi Walled Carbon Nano Tubes (MWCNTs) Nano- Composites. *Int. J. Light. Mater. Manuf.* **2020**, *4*, 195–202. [CrossRef]
6. Can, A.; Kaya, F.; Kaya, C. A study on optimum surfactant to multiwalled carbon nanotube ratio in alcoholic stable suspensions via UV—Vis absorption spectroscopy and zeta potential analysis. *Ceram. Int.* **2020**, *46*, 29120–29129. [CrossRef]
7. Fujimori, T.; Morelos-Gómez, A.; Zhu, Z.; Muramatsu, H.; Futamura, R.; Urita, K.; Terrones, M.; Hayashi, T.; Endo, M.; Young Hong, S.; et al. Conducting linear chains of sulfur inside carbon nanotubes. *Nat. Commun.* **2013**, *4*, 2162. [CrossRef] [PubMed]
8. Aftab, J.; Mehmood, S.; Ali, A.; Ahmad, I.; Bhopal, M.F.; Rehman, M.Z.U.; Shah, M.Z.U.; Shah, A.U.; Wang, M.; Khan, M.F.; et al. Synergetic Electrochemical Performance of Tungsten Oxide/Tungsten Disulfide/MWCNTs for High-Performance Aqueous Asymmetric Supercapattery Devices. *J. Alloys Compd.* **2023**, *965*, 171366. [CrossRef]
9. Isacfranklin, M.; Yuvakkumar, R.; Kungumadevi, L.; Ravi, G.; Rajendran, V. Boron, Nitrogen, Sulfur Heteroatom Influence Effect on Direct Growth Carbon Nanotubes on Ni Foam for Anode Electrodes. *Electrochim. Acta* **2023**, *468*, 142961. [CrossRef]
10. Stuart, B.H. *Infrared Spectroscopy: Fundamentals and Applications*; John Wiley & Sons: Hoboken, NJ, USA, 2005. [CrossRef]
11. Rasheed, H.K.; Kareem, A.A. Effect of Multiwalled Carbon Nanotube Reinforcement on the Opto-Electronic Properties of Polyaniline/c-Si Heterojunction. *J. Opt. Commun.* **2021**, *42*, 25–29. [CrossRef]
12. Infrared Spectroscopy. Available online: <https://www2.chemistry.msu.edu/faculty/reusch/virttxtjml/spectrpy/infrared/infrared.htm> (accessed on 2 July 2023).
13. Shuit, S.H.; Tan, S.H. Feasibility study of various sulphonation methods for transforming carbon nanotubes into catalysts for the esterification of palm fatty acid distillate. *Energy Convers. Manag.* **2014**, *88*, 1283–1289. [CrossRef]
14. Patodia, T.; Sharma, K.B.; Dixit, S.; Katyayan, S.; Agarwal, G.; Jain, A.; Jain, S.K.; Tripathi, B. Carbon nanotube-sulfur nanocomposite electrodes for high energy-foldable lithium sulfur battery. *Mater. Today Proc.* **2019**, *42*, 1638–1641. [CrossRef]
15. Jadhav, C.D.; Pandit, B.; Karade, S.S.; Sankapal, B.R.; Chavan, P.G. Enhanced field emission properties of V₂O₅/MWCNTs nanocomposite. *Appl. Phys. A Mater. Sci. Process.* **2018**, *124*, 794. [CrossRef]

Disclaimer/Publisher’s Note: The statements, opinions and data contained in all publications are solely those of the individual author(s) and contributor(s) and not of MDPI and/or the editor(s). MDPI and/or the editor(s) disclaim responsibility for any injury to people or property resulting from any ideas, methods, instructions or products referred to in the content.